Polymer Chemistry

Accepted Manuscript

This article can be cited before page numbers have been issued, to do this please use: J. Xu, H. Zhou, X. Wang, T. T. Lin, J. Song and B. Z. Tang, *Polym. Chem.*, 2016, DOI: 10.1039/C6PY01358A.

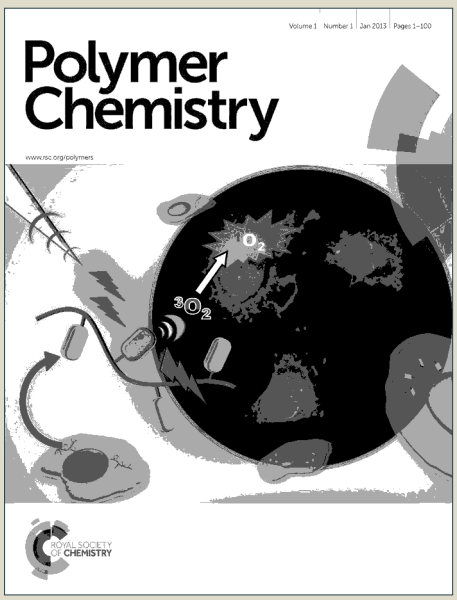

ROYAL SOCIETY OF CHEMISTRY

www.rsc.org/polymers

View Article Online
DOI: 10.1039/C6PY01358A

Journal Name

ARTICLE

Poly(triphenyl ethene) and poly(tetraphenyl ethene): Synthesis, aggregation-induced emission property and application as paper sensors for effective nitro-compounds detection†

Received 00th January 20xx,
Accepted 00th January 20xx

DOI: 10.1039/x0xx00000x

www.rsc.org/

Hui Zhou,[a] Xiaobai Wang,[a] Ting Ting Lin,[a] Jing Song,[a] Ben Zhong Tang*[b] and Jianwei Xu*[ac]

Two unique aggregation-induced emission (AIE) active polymers poly(triphenyl ethene) **(PTriPE**) and poly(tetraphenyl ethene) (**PTPE)**, comprising sole repeating units triphenyl and tetraphenyl, respectively, were synthesized through Suzuki coupling of (2,2-dibromoethene-1,1-diyl)dibenzene and related di-boronic acid or ester compounds. The polymers **PTriPE** and **PTPE** had number-molecular weights (10,100-17,400) with polydispersity indices of 1.5-1.7, and they were soluble in common organic solvents. The polymers in THF/H_2O mixtures were able to form remarkably stable nanoparticles and no agglomeration was observed even when stored at 4 ^{o}C for several months. The polymer **PTriPE** and **PTPE** exhibited much more significant AIE activities when compared to their corresponding small AIE molecule 1,1,2,2-tetraphenylethene (**TPE**) and 4,4'-(2,2-diphenylethene-1,1-diyl)dibiphenyl (**DPDB**) in THF-H_2O mixtures. The fluorescence of polymer nanoparticles in THF/H_2O mixture could be significantly quenched by various nitro-compounds, and **PTriPE** nanoparticles demonstrated better fluorescence quenching response than **PTPE**. The film formed by **PTriPE** nanoparticles showed reasonable fluorescence quenching response to nitro-compounds, for example, ~ 5 ppb in the case of 2,4,6-trinitrotoluene vapor, despite its thickness approaching to a micrometer level. Futhermore, **PTriPE**-based paper sensors were fabricated from its polymer nanoparticles solution, and is still effective with a polymer surface concentration of low down to 1.0 μg·cm^{-2} in detecting various nitro-compounds in a scale of less than 1 ng, making it a useful tool to offer a quick, inexpensive and most importantly highly sensitive detection for nitro-compounds based explosives.

Introduction

Explosives detection has been becoming an increasingly crucial task for public security and cumulative worldwide terrorism thereat. Nitro-substituted organic compounds are a common class of highly-explosive chemicals, and nitro-aromatics, especially 2,4,6-trinitrotoluene (TNT), are the major military explosives and abused worldwide. Various instrumental analytical methodologies have been developed for the explosive detection.[1-7] For example, the Environmental Protection Agency (EPA) protocol SW-846 Method 8330a involves the use of reverse-phase HPLC with UV detection. However, these detection methods are always very costly and time-consuming, and more importantly, are not portable for on-site detection.

Fluorescence technology has been received much attention for explosive detection in the past few decades, due to its ultra-high sensitivity, high efficiency.[8-10] Thin films fabricated from conjugated polymers are applied for the vapor detection of explosives due to their exciton migration effects.[11] However, the performance of most thin film is restricted by its dependence on thickness, due to the fact that diffusion of analyte vapor in poorly porous rigid films is extremely slow.[12] A pentiptycene-based polymer film with thickness of 2.5 nm shows near 4-fold higher fluorescence quenching efficiency on TNT vapor than that of thicker film (25 nm).[12a] A lot of research groups have been attempting to solve this issue by increasing the porosity of the film. We have also demonstrated that porous films obtained by electrospinning AIE active copolymers show strong response to vapor of nitro-compounds.[13] Unlike the films fabricated from common fluorescent conjugated polymers, the porous films of AIE active polymer exhibit less dependence of quenching efficiency on film thickness despite thickness as high as several hundred nanometers.[13]

Herein, we reported two structurally exceptional polymers entirely constructed by commonly-used AIE active moieties TPE or triphenyl without including any linkages, co-monomers or flexible chains. To our knowledge, these two polymers are surprisingly not reported although a huge number of TPE-containing copolymers have been synthesized.[14] These two polymers were readily synthesized though Suzuki coupling reaction and their fluorescence

[a]*Institute of Materials Research and Engineering, Agency for Science, Technology and Research (A*STAR), 2 Fusionopolis Way, Innovis, #08-03, Singapore 138634. E-mail: jw-xu@imre.a-star.edu.sg*
[b]*Department of Chemistry, The Hong Kong University of Science & Technology, Clear Water Bay, Kowloon, Hong Kong, China. E-mail: tangbenz@ust.hk*

View Article Online
DOI: 10.1039/C6PY01358A

quenching response to nitro-compounds was studied. The paper sensors fabricated by absorbing the polymer nanoparticles onto a piece of filter paper showed high sensitivity for contamination of solid nitro-compound particles, hence, providing a useful tool to detect nitro-compound contamination for practical applications.

Results and Discussion

Synthesis and characterization of polymer

The synthetic routes leading to **PTriPE** and **PTPE** are shown in Scheme 1. The starting material (2,2-dibromoethene-1,1-diyl)dibenzene (**1**) was prepared from benzophenone and tetrabromomethane according to reference.[15] **PTriPE** and **PTPE** were prepared from a mixture of compound **1** and a related diboronic acid or diboronic ester through the Suzuki coupling reaction with reasonable yields of 76% and 74%, respectively. The **PTriPE** and **PTPE** were obtained by re-precipitation twice in methanol, followed by Soxhlet extraction with different solvents, including hexane, Et_2O and MeOH. They are soluble in most organic solvents, such as tetrahydrofuran (THF), dichloromethane, chloroform, etc. The molecular weights of those two polymers were determined by gel permeation chromatography (GPC) using polystyrene as the standards and the data are listed in Table 1. The polymers show reasonable molecular weights of 15,200 and 29,600 Dalton with polydispersity index of 1.5 and 1.7, respectively. **PTriPE** and **PTPE** displayed high thermal stability with T_d around 400 °C under N_2 (Fig. S1).

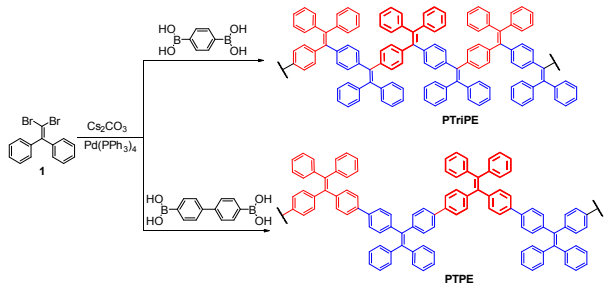

Scheme 1 Structure illustration of polymer **PTriPE** and **PTPE**.

Table 1. Properties of **PTriPE** and **PTPE**.

Unit	Yield (%)	M_w (10^{-3})	M_n (10^{-3})	PDI	T_d (in N_2)	T_g (in N_2)
PTriPE	76	15.2	10.1	1.5	402	163
PTPE	74	29.6	17.4	1.7	400	193

M_w = mass average molar mass, M_n = number average molar mass, PDI = polydispersity index, T_d = decomposition temperature, T_g = glass transition temperature.

Aggregation-induced emission

PTriPE and **PTPE** were almost non-emissive when dissolved in THF. As shown in Fig. S2, when compared with small molecules **TPE** and **DPDB**, the significant redshifts by 21 nm and 42 nm in the UV-vis spectrum are observed for **PTriPE** and **PTPE** respectively, due to the longer conjugated structure in polymers. The fluorescence of polymers would be turned on by addition of poor solvents such as H_2O. As shown in Fig. 1, **PTriPE** started to be emissive obviously when the H_2O content was more than 40%. In contrast, monomeric **TPE** only emitted week fluorescence when the H_2O content reaches 80%. **PTriPE** emitted stronger fluorescence by 38.3-fold than **TPE** with the same weight percentage in the THF/H_2O (1:9 v/v) (Fig. S3c).

The mixtures of polymer in THF/H_2O were visually transparent without any precipitations. The polymer particles started to form when H_2O content is 10%, and the particle sizes were gradually reduced from 1250 to 300 nm until H_2O content reaches 90% (Fig. 2a). This observation is consistent with the AIE mechanism, in which the stronger aggregation of particle leads to stronger fluorescence. The fluorescence quantum yields of polymers are summarized in Table 2. **PTriPE** and **PTPE** in THF exhibit negligibly small Φ_f values, being 0.04% and 0.74% respectively. In the mixture of THF/H_2O (1 : 9 v/v), the Φ_f values of **PTriPE** and **PTPE** rise up to 14.39% and 18.07% respectively, which are lower than the reported Φ_f values of TPE-containing conjugated polymers (18%, 28% and 64%).[14c] The lower Φ_f efficiencies may be resulted from planarization effect. Typically, conjugated materials prefer to form planar conformation in the excited state compare to their ground state. However, as shown in Fig. 4, the optimized polymer structures exhibit a highly twisted geometry even in the excited state, in which the steric effect of the neighbouring bulky phenyl groups inhibit planarization of the polymer structure, leading to relatively low Φ_f efficiencies.[16a]

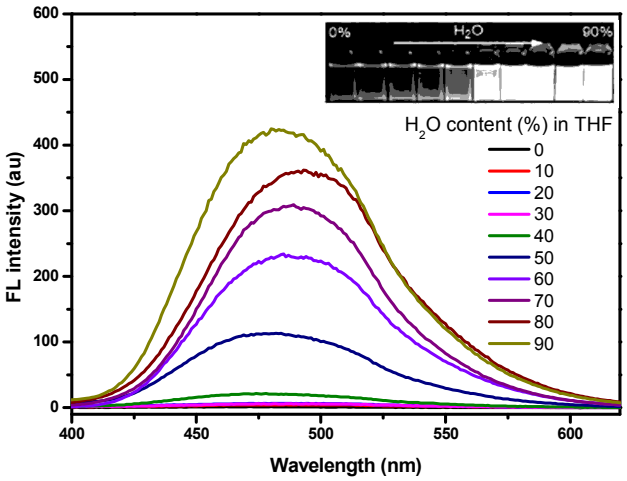

Fig. 1 Fluorescence spectra of **PTriPE** in THF/H_2O mixtures with different H_2O contents (λ_{ex} = 332 nm, [**PTriPE**] = 100.0 μg·mL^{-1}, inserted photos are **PTriPE** solutions taken under UV radiation (λ_{ex} = 365 nm)).

View Article Online
DOI: 10.1039/C6PY01358A

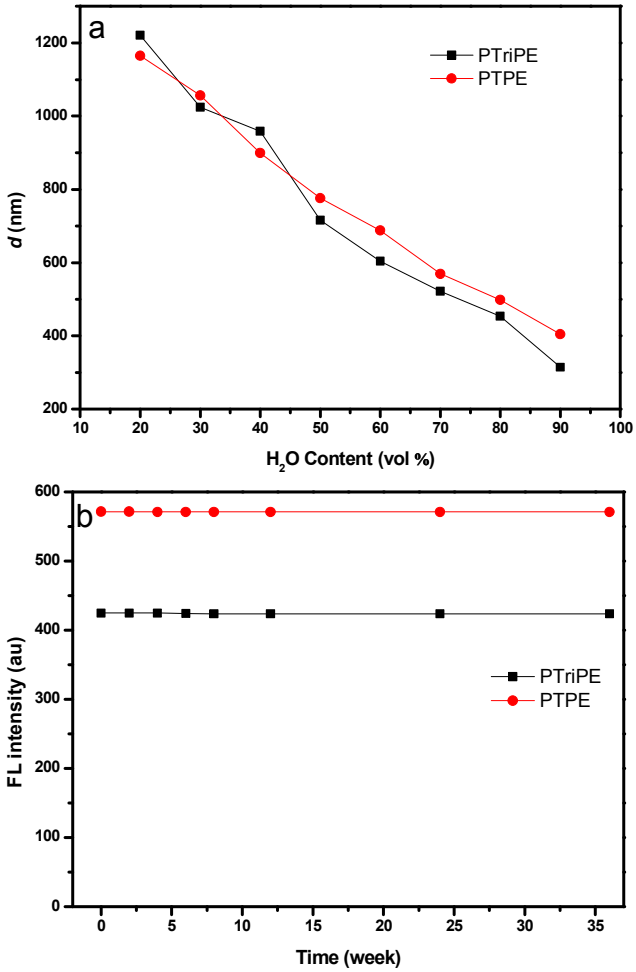

Fig. 2 (a) The particle size (d) of polymer in THF/H_2O mixtures measured by dynamic light scattering (DLS). Turbidity data measured as a function of absorbance at 633 nm, [C] = 100.0 μg·mL^{-1}. (b) The fluorescence intensity of polymer nanoparticles in THF/H_2O (1:9 v/v) mixture *via* time. Samples were stored at 4 °C, [C] = 100.0 μg·mL^{-1}.

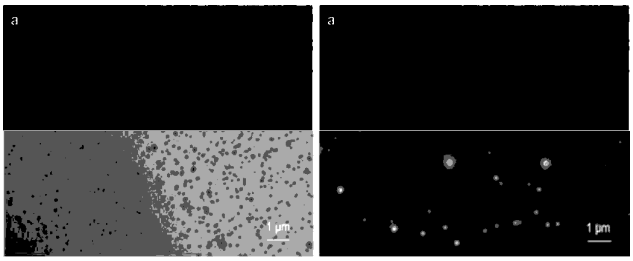

Fig. 3 The enlarged image (a) and fluorescent image (b) of polymer nanoparticles. Samples prepared from polymer in THF/H_2O (1:9 v/v) mixture, [**PTriPE**] = 100.0 μg·mL^{-1}. The fluorescent image of polymer nanoparticles is taken under a fluorescence microscope with a 337 nm excitation.

Electrochemistry

The electrochemistry of **PTriPE** and **PTPE** were studied by cyclic voltammetry (CV) using a three-electrode system with $LiClO_4$ solution in anhydrous THF (0.1 M). The glassy carbon was used as the working electrode, the platinum wire was the counter electrode, and the Ag/Ag^+ was the reference electrode (0.1 M). As shown in Table 2, the HOMO levels of **PTriPE** and **PTPE** were calculated to be -5.50 and -5.66 eV using the reported equation $-(E_{ox} + 4.70)$,[16] in which the E_{ox} of **PTriPE** and **PTPE** were found to be 0.80 and 0.96 eV. Thus, the band gaps of **PTriPE** and **PTPE** were calculated from their onset wavelengths of UV absorption to be 3.08 and 3.12 eV, respectively.

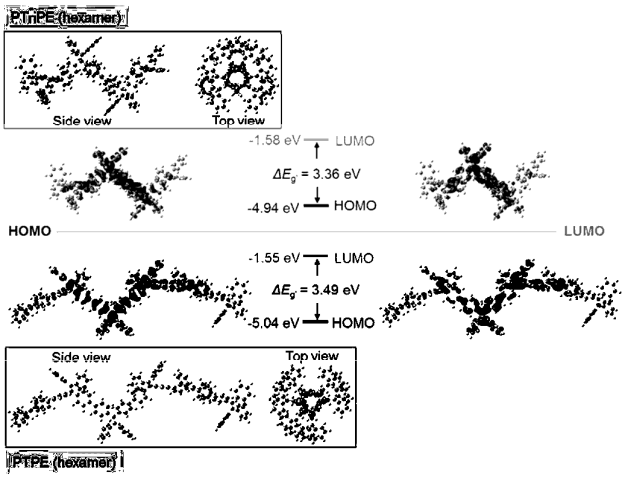

Fig. 4 Optimized molecular structures and molecular orbital amplitude plots of HOMO and LUMO energy levels of the **PTriPE** and **PTPE** calculated using the B3LYP/6-31G(d,p) basis set.

Table 2. Optical and electrochemical properties of **PTriPE** and **PTPE**.

Unit	λ_{ab} (nm)	λ_{ex} (nm)	Φ_f^{soln} (%)	Φ_f^{aggre} (%)	$E_{ox}{}^a$ (eV)	HOMO	LOMO	$E_g{}^b$ (eV)
PTriPE	332	493	0.04	14.39	0.80	-5.50	-2.42	3.08
PTPE	334	480	0.74	18.07	0.96	-5.66	-2.54	3.12

λ_{ab} = absorption in THF, λ_{ex} = emission maximum in THF/H_2O (1:9 v/v), λ_{onset} = onset absorption wavelength, Φ_f^{soln} = FL quantum yields in THF, Φ_f^{aggre} = quantum yield in THF/H_2O (1:9 v/v), [C] = 1×10^{-5} M. $^aE_{ox}$ = onset oxidation potential measured by CV. HOMO = $-(E_{ox} + 4.70)$.[16] ^{b}The data were calculated by the equation: $E_g = 1240/\lambda_{onset}$, LUMO = HOMO + E_g.

The structures of oligomers **PTriPE** and **PTPE** were modulated using density functional theory (DFT). As shown in Fig. 4, the HOMO of **PTriPE** is dominated by the TPE orbitals, and the TPE units are conjugated each other. However, when the repeating units of the oligomer are increased to hexamer, their phenyl rings contribute weakly to the HOMO energy levels. All the oligomers have similar LUMO, which are also dominated by the TPE orbitals. The DFT calculated energy

View Article Online
DOI: 10.1039/C6PY01358A

band gaps of hexamers (3.36 and 3.49 eV) are higher than that of experimental values (3.08 and 3.12 eV), which may indicate that the longer conjugation structures exist in **PTriPE** and **PTPE** than DFT modulated.

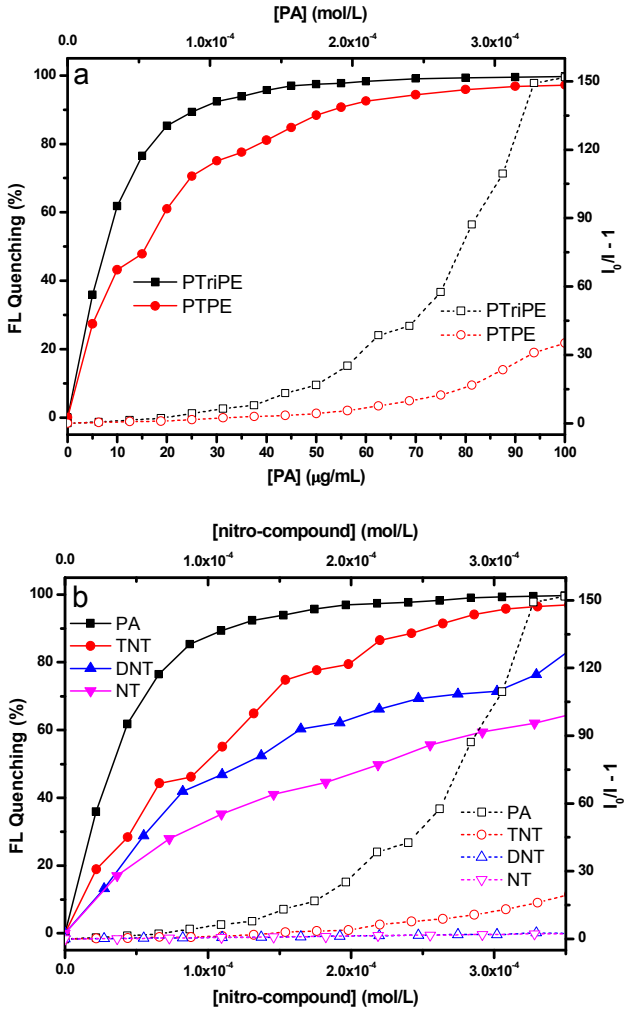

Fig. 5 (a) Concentration-dependent fluorescence quenching of **PTriPE** and **PTPE** by PA. (b) Concentration-dependent fluorescence quenching of **PTriPE** by nitro-compounds. [Polymer] = 100.0 μg·mL^{-1} in THF/H_2O (1:9 v/v) mixture.

Fluorescence quenching of polymer nanoparticles by nitro-compounds

The polymer nanoparticles of **PTriPE** in THF/H_2O mixture emitted strong fluorescence in the range of 400-600 nm centred at 480 nm (Fig. 1 and Fig. 3). The fluorescence quenching of the polymer was due to electron-transfer between the polymer and nitro-compounds. Nitro-compounds with a relatively low LUMO energy level can accept an exited state electron from the polymer, and thus quench fluorescence of the polymer. In this case, PA was first chosen as an analyte in the fluorescence quenching experiment due to its lowest LUMO energy among common nitroaromatics. Significant fluorescent quenching for **PTriPE** was observed after adding PA ([PA] = 0 – 100 μg·mL^{-1}) in THF/H_2O immediately (Fig. 5a). The fluorescence quenching efficiency reaches to 97% when the PA concentration is up to 50 μg·mL^{-1}. When the PA concentration is less than 40 μg·mL^{-1}, the Stern-Volmer plots of **PTriPE** is almost linear with a quenching constant of 1.80 × 10^5 M^{-1}, which is almost 10-fold higher than 1.22 × 10^4 M^{-1} of **PTPE** and also much higher than that of reported polymers (4.27-9.72 × 10^4 M^{-1}).[10a] In addition, the quenching constant of **PTriPE** for TNT, DNT and NT are 2.56 × 10^4, 6.70 × 10^3 and 6.65 × 10^4 M^{-1}, respectively (Fig. 5b), which are also much higher than that of **PTPE** (Fig. S4). The larger fluorescence quenching response of **PTriPE** to nitro-compounds is due to its higher LUMO energy level than that of **PTPE** and thus a larger driving force of 1.47 eV for **PTriPE** than that of 1.35 eV for **PTFE** (*vide infra*).

Electrospun film for detection of nitro-compounds vapours

Electrospinning is a useful method to prepare both polymer particles and fibres with diameters ranging from nanometers to micrometers.[17] Typically, the morphology of formed substrates was affected by preparation conditions and physicochemical properties of polymer solutions.[18] In present study, we were motivated to fabricate porous films by electrospinning solution of polymer in acetone/chloroform co-solvent.

Table 3. Properties of **PTriPE**, **PTPE** and their corresponding films.

Polymer	Film	Fabrication method	Thickness (μm)[a]
PTriPE	F1	Drop coating	5.51±0.36
PTriPE	F2	Spin coating	2.00±0.24
PTriPE	F3	Electropun	1.61±0.06
PTPE	F4	Electropun	1.54±0.16

[a]Experiments were performed in duplicate and mean values were taken.

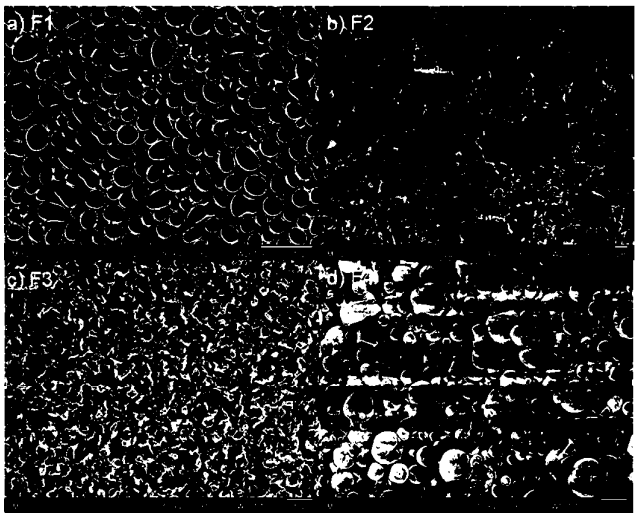

View Article Online
DOI: 10.1039/C6PY01358A

Fig. 6 SEM images of films: (a) F1, (b) F2, (c) F3 and (d) F4, scale bar is 10 µm. See processing parameters in Table S1.

The films F1-4 were prepared from polymers solutions with 2.0 wt% in acetone/chloroform mixture (1/1, v/v) *via* drop-coating, spin-coating and electrospinning, respectively. The film morphology was checked by SEM as shown in Fig. 6. F1 displays a porous structure with holes ranging from 2 to 4 µm, which may be formed by the evaporation of solvents. In contrast, F2 only shows a cracked surface. F3 and F4 were fabricated by electropsun of **PTriPE** and **PTPE** respectively. In both cases, SEM images showed crumpled particles or particles with different size, which are different morphologies from theses obtained from drop coating and spin coating. However, the polymer fibres with uniform nanostructure cannot be obtained although we attempted to tune the electrospinning parameters, such as needle gauge, flow rate, voltage, and distance between needles. **PTriPE** film prepared by electrospinning exhibits a S_{BET} value of 120 m^2/g, which is near 20-fold larger than that of **PTriPE** film prepared from drop casting (S_{BET} = 6 m^2/g) (Fig. S5). The obvious increase in S_{BET} value suggests that the porous structure can be efficiently fabricated by electrospinning, being consistent with the observation by SEM images.

After exposing to DNT vapour (Fig. 7a), fluorescence quenching was found immediately for porous film F3, and the quenching efficiency reached to 25% in 30 s, 68% in 2 min and 75% in 4 min. At the same condition, the quenching efficiencies of other films are all less than 28% in 4 min (Fig. 7b). Therefore, high porous film F3 has faster fluorescence response than other low porous films, which is consistent with our previous observations that the porous structure could facilitate the diffusion of the gaseous analytes inside the polymer film, thereby improving its sensitivity.[13] However, F3 responded sluggishly to TNT vapour, and its quenching efficiency reached 18% in 30 s, 35% in 4.0 min and 69% in 20 min (Fig. 7c). The smaller quenching efficiency to TNT vapour may be due to its lower vapour concentration (ca. 5 ppb) than DNT (ca. 100 ppb). The quenching efficiency for NT vapour is only 15% in 4 min, while no response to toluene vapour, indicating F3's good sensing selectivity to vapour of nitro-compounds.

Comparing to the fluorescence quenching efficiency of reported conjugated polymers,[11j-l,12a,12e,14a] non-conjugated polymers[13] and macromolecules,[19] **PTriPE** film shows reasonable fluorescence quenching efficiency to TNT and DNT vapours although its thickness is several hundred folds more than that of reported polymers, indicating its less dependence of quenching efficiency on the film thickness. This may relate to the twisted structure of polymers, which easily bind with nitro-compounds and thus enhance the fluorescence quenching.[12a]

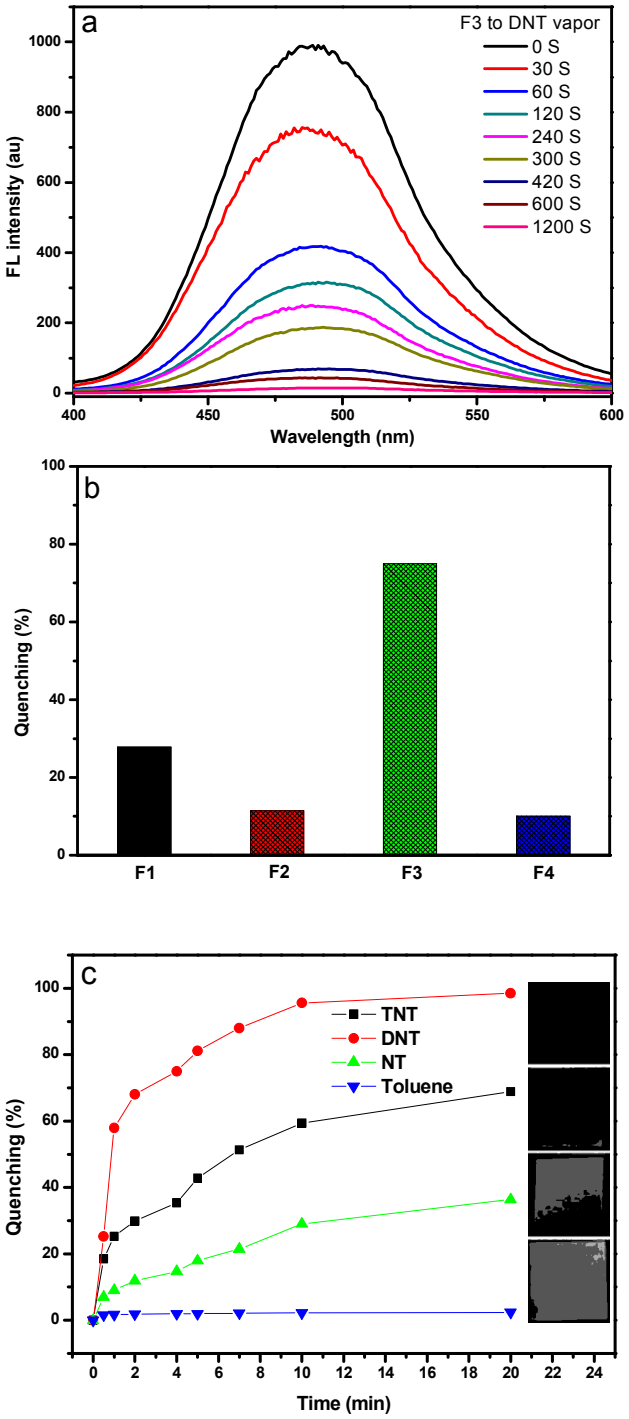

Fig. 7 (a) Fluorescence quenching of F3 on exposure to DNT saturated vapour. (b) Fluorescence quenching of films F1-F6 on exposure to DNT saturated vapour for 4.0 min, 25 °C. (c) Time-dependent fluorescence quenching of porous film F3 on exposure to saturated vapour of TNT, DNT, NT and toluene, respectively. The inserted photos are F3 on exposure to analytes saturated vapour under UV light (365 nm) radiation, 25 °C.

View Article Online
DOI: 10.1039/C6PY01358A

Paper sensor for nitro-compounds detection

For the further real application of nitro-compounds detection, a piece of Whatman filter paper was fabricated by spray-coating a polymer nanoparticles solution on the filter paper through air brush, wherein polymer nanoparticles was prepared in THF/H_2O (1:9 v/v). After dry completely, the filter paper was placed under UV light (λ_{ex} = 365 nm) to check its fluorescence. Fig. 8 shows the fluorescent images of paper sensor, accounting a surface concentration of polymer nanoparticles approximately as 2.0, 1.0, 0.5, 0.25 and 0.125 μg·cm^{-2}, respectively. Among of them, the paper sensor with surface concentration of 1.0 μg·cm^{-2} exhibited strong fluorescence without defect spots, and was selected for the next test.

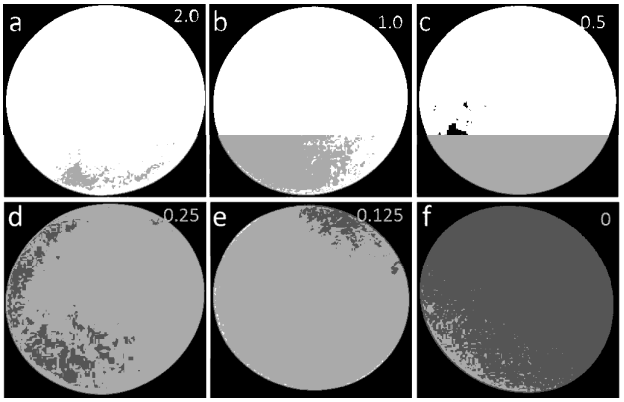

Fig. 8 The images of paper sensor under UV light (365 nm), which was prepared by spray-coating polymer nanoparticles of **PTriPE** in THF/H_2O (1:9 v/v) mixture onto filter paper, amounting to approximately concentration as: (a) 2.0 μg/cm^2; (b) 1.0 μg/cm^2; (c) 0.5 μg/cm^2; (d) 0.25 μg/cm^2; (e) 0.125 μg/cm^2; (f) 0 μg/cm^2.

Comparing to the **PTriPE** porous film (F3) prepared by electrospinning, the paper sensor responded sluggishly to the vapor of nitro-compounds (Fig. S8-10). For example, the fluorescence of paper sensor was not totally quenched even exposure to DNT statured vapor for 30 min. However, the paper sensor is effective for the detection of a trace amount of nitro-compounds. Fig. 9a demonstrates the nitro-compounds detection by depressing the finger (nitrile gloved) with nitro-compounds contamination to the paper sensor. Trace amounts of nitro-compound were analysed after the contaminated finger was contacted with a solid nitro-compound. Taking PA an example, the right finger was rubbed with PA powder and then wiped with tissue paper till no visible PA particulates were left, and the left finger remained clean for comparison. The right finger contaminated with a trace amount of PA, and uncontaminated left finger then simultaneously touched onto the same paper sensor for a very short period (~ 1s). The fluorescence of contaminated paper sensor was checked immediately under UV illustration (365 nm), and fluorescence quenching was clearly observed by naked eyes in a place touched by the contaminated finger (Fig. 9c). Moreover, as shown in Fig. 9d-f, other contaminated fingers by TNT, DNT and NT were positively identified through fluorescence quenching.

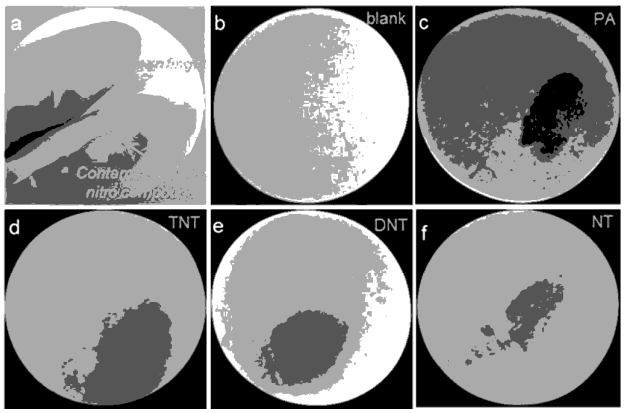

Fig. 9 The demonstration for nitro-compounds contamination detection; the fluorescent images were checked by naked eyes immediately after depression of gloved finger that was contaminated by nitro-compounds solid in trace scale. (a) The bright image of paper sensor with clean finger and contaminated finger printing. (b) The image of paper sensor under UV light (365 nm) without nitro-compound. (c), (d), (e) and (f) are the images of paper sensor under UV light (365 nm) after finger printing with PA, TNT, DNT and NT, respectively.

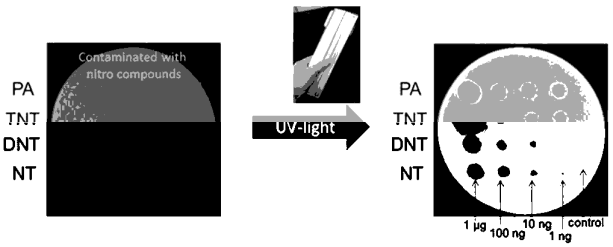

Fig. 10 The detection limit of paper sensor on nitro-compounds. The images of paper sensor are under UV light radiation (365 nm). Nitro-compounds are PA, TNT, DNT and NT.

Finally, the detection limit of paper sensor for nitro-compounds was obtained as shown in Fig. 10. Aliquots of nitro-compound stock solutions were syringed onto Whatman filter paper (d = 55 mm). The sizes of spot were between 2 and 5 mm in diameter, to produce a surface concentration ranging from 34-128 ng·cm^{-2}. Finally, the surface concentration of nitro-compounds on the filter paper were controlled as 1 000, 100, 10 and 1 ng·cm^{-2}, respectively. Then, a layer of polymer nanoparticles, with a surface concentration approximately 1.0 μg·cm^{-2} was fabricated to the contaminated filter paper via spray-coating polymer nanoparticles in THF/H_2O (1:9 v/v, 1.0 μg·mL^{-1}), and allowed to dry completely. The coated filter paper was placed under UV light (λ_{ex} = 365 nm) to check the

View Article Online
DOI: 10.1039/C6PY01358A

fluorescence of paper sensor. Dark spots on the paper sensor indicated fluorescence quenching by nitro-compounds. The dark spots were still very obvious even the analyte weight of 1 ng, indicating the good detecting sensitivity of paper sensor to nitro-compounds.

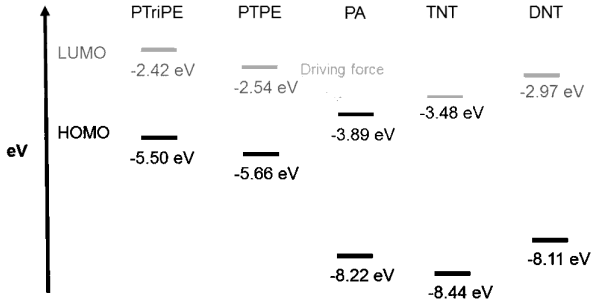

Fig. 11 HOMO and LUMO energy levels of the PTriPE and PTPE with various explosive analytes.[20]

Conclusions

Two polymers **PTriPE** and **PTPE** fully built by **TriPE** and **TPE**, respectively, were first prepared and their AIE properties were examined. **PTriPE** and **PTPE** exhibited typical AIE properties in THF/water and their films with a few micrometers thickness were fabricated by different methods. Polymer **PTriPE** film fabricated by electronspinning showed better response to nitro-aromatics in the order of DNT, TNT and NT than **PTPE.** Compared to the reported conjugated polymers for detection of nitro-compounds, **PTriPE** demonstrated less dependence of quenching efficiency on the film thickness. In addition, porous film formed *via* electrospinning exhibited significantly improved fluorescence quenching efficiency to nitro-compounds than their corresponding dense films. Furthermore, a **PTriPE**-based paper sensor prepared by absorbing polymer nanoparticles onto a piece of porous filter paper displayed very low detection limit even though the analyte scale was low down to 1.0 ng, revealing its potential practical application in detection of nitro-aromatics. The paper sensors are effective in detecting not only the nitro-compounds with high-vapor pressure, such NT, DNT, but also nitro-compounds with low-vapour pressure, such as TNT, PA. Thus, this type of paper sensors would offer a quick, inexpensive and highly sensitive detection method for nitro-compounds-based explosives.

Experimental section

Materials

TNT was prepared from DNT according to reference.[10a] PA and DNT were purchased from Aldrich. (2,2-dibromoethene-1,1-diyl)dibenzene (**1**) was prepared from benzophenone and tetrabromomethane according to reference.[15] **TPE** was prepared according to reference.[15]

Instrumentation

^{1}H and ^{13}C NMR spectra were obtained on a Bruker DRX 400-MHz NMR spectrometer (400.13 MHz for ^{1}H and 100.61 MHz for ^{13}C) in $CDCl_3$ at 25 ^{o}C. All peaks are reported in ppm using tetramethylsilane (TMS) as an internal standard (0 ppm). MALDI-TOF spectrum was obtained on a Bruker Autoflex III TOF/ TOF. Elemental analysis was performed on a Perkin-Elmer 240C elemental analyser. Thermal properties of polymer were analysed on a Perkin-Elmer thermogravimetric analyzer 7 *via* heating rate of 20 ^{o}C/min, and on a TA Instruments Differential Scanning Calorimetry 2920 *via* heating/cooling rate of 20 ^{o}C/min in N_2. The particle sizes in solution were obtained on a Brookhaven zetaplus spectrometer with a light source of 633 nm argon ion laser. UV-vis and fluorescence spectra were performed on a Shimadzu UV3101PC UV-vis spectrophotometer and a Shimadzu fluorescence spectrometer, respectively. The Φ_f of materials were calculated based on 1×10^{-5} M quinine sulphate solution in 0.1 M H_2SO_4 (Φ_f = 0.55). The gas adsorption isotherms were measured on an ASAP 2020 surface area analyser. The fluorescent image of polymer nanoparticles is taken under a Nikon Polarizing Microscope LV100POL.

Electrohydrodynamic preparation

The solutions of polymer for electrospinning were formed though dissolving polymer in mixture of chloroform and acetone (1:1 v/v), and filtered by 0.2 μm filter before using. Processing parameters for electrospinning are listed in Table S1. The resulting polymer substrates were place in an oven to vacuum dry at 25 ^{o}C for 24 hours before test.

Synthesis of compounds and polymers

4,4'-(2,2-diphenylethene-1,1-diyl)dibiphenyl (**DPDB**). (2,2-dibromoethene-1,1-diyl)dibenzene (67.6 mg, 0.20 mmol), [1,1'-biphenyl]-4-ylboronic acid (87.1 mg, 0.44 mmol), K_2CO_3 (276.0 mg, 2.00 mol) and $Pd(PPh_3)_4$ (23.1 mg, 0.02 mmol) were placed in a Schlenk flask. Toluene (2.0 mL), ethanol (0.5 mL) and H_2O (0.5 mL) was added, then the mixture was degassed with N_2 for 30 min and stirred at 105 ^{o}C under N_2 for overnight. After cooling down, the reaction mixture was poured into H_2O, extracted by dichloromethane (2 × 50.0 mL). The organic phase was collected and dried over Na_2SO_4, filtered, and evaporated. The crude product was purified by chromatography over silica gel eluting with hexane/dichloromethane (8:1 v/v), giving product as an light yellow solid 73 mg (75%). ^{1}H NMR ($CDCl_3$): δ 7.56 (d, 4H, J = 8.3 Hz), 7.38 (m, 8H), 7.31 (m, 2H), 7.11 (m, 14H). ^{13}C NMR ($CDCl_3$): δ 144.2, 143.2, 141.1, 139.3, 132.3, 131.8, 129.1, 128.2, 127.6, 127.3, 126.9, 126.6. MALDI-TOF: [M] calcd for $C_{38}H_{28}$, m/z 484.22; found, m/z 484.35. IR (thin film): ν = 3051, 3029, 2919, 2848, 1618, 1570, 1520, 1478, 1415, 1360, 1198, 862, 827, 757, 720, 694 and 578 cm^{-1}. Anal. Calcd for $C_{38}H_{28}$: C, 94.18; H, 5.82. Found: C, 94.09; H, 5.93.

Poly(triphenyl ethene) (**PTriPE**). (2,2-dibromoethene-1,1-diyl)dibenzene (338.04 mg, 1.00 mmol), 1,4-phenylenediboronic acid (165.75 mg, 1.00 mmol), K_2CO_3 (0.69 g, 5.00 mol) and $Pd(PPh_3)_4$ (57.85 mg, 0.05 mmol) were placed in a Schlenk flask. Toluene (16.0 mL), ethanol (4.0 mL) and H_2O

View Article Online
DOI: 10.1039/C6PY01358A

(4.0 mL) was added, then the mixture was degassed with N_2 for 30 min and stirred at 105 °C under N_2 for overnight. After cooling down, the reaction mixture was poured into H_2O, extracted with dichloromethane (2 × 50.0 mL). The organic phase was collected and dried over Na_2SO_4, filtered, and evaporated. The crude product was first purified by precipitating its solution in THF (2 mL) by methanol (100 mL). Then the solid was collected by filtration, and was further purified by Soxhlet extraction with hexane, methanol and Et_2O, giving **PTriPE** as a yellow powder (190.0 mg, 75%). ^{1}H NMR ($CDCl_3$): δ 7.09-6.97 (m, 12H), 6.73-6.69 (m, 2H). ^{13}C NMR ($CDCl_3$): δ 144.0, 131.6, 131.5, 130.8, 130.7, 128.3, 127.9, 127.7, 126.6, 126.5. IR (thin film): ν = 3027, 2919, 2848, 1595, 1559, 1498, 1481, 1424, 1360, 1215, 1022, 871, 764, 735, 707, 641 and 571 cm^{-1}. Anal. Calcd for $(C_{20}H_{14})_n$: C, 94.45; H, 5.55. Found: C, 94.39; H, 5.63.

Poly(tetraphenyl ethene) (**PTPE**). (2,2-dibromoethene-1,1-diyl)dibenzene (338.04 mg, 1.00 mmol), 4,4'-bis(4,4,5,5-tetramethyl-1,3,2-dioxaborolan-2-yl)-1,1'-biphenyl (406.14 mg, 1.00 mmol), K_2CO_3 (0.69 g, 5.00 mol) and $Pd(PPh_3)_4$ (57.85 mg, 0.05 mmol) were placed in a Schlenk flask. Toluene (16.0 mL), ethanol (4.0 mL) and H_2O (4.0 mL) was added, then the mixture was degassed with N_2 for 30 min and stirred at 105 °C under N_2 for overnight. After cooling down, the reaction mixture was poured into H_2O, extracted with dichloromethane (2 × 50.0 mL). The organic phase was collected and dried over Na_2SO_4, filtered, and evaporated. The crude product was first purified by precipitating its solution in THF (2 mL) by methanol (100 mL). Then the solid was collected by filtration, and was further purified by Soxhlet extraction with hexane, methanol and Et_2O, giving PTPE as a yellow powder (242 mg, 73%). ^{1}H NMR ($CDCl_3$): δ 7.66 (m, 1H), 7.33 (m, 5H), 7.08 (m, 11H), 6.90 (m, 1H). ^{13}C NMR ($CDCl_3$): δ 144.2, 143.2, 138.7, 132.2, 131.8, 130.8, 129.1, 128.6, 128.4, 128.2, 128.0, 127.9, 127.6, 126.9, 126.6, 126.3. IR (thin film): ν = 3049, 3018, 2922, 2852, 1597, 1568, 1514, 1442, 1357, 1074, 1029, 854, 752, 628 and 576 cm^{-1}. Anal. Calcd for $(C_{26}H_{18})_n$: C, 94.51; H, 5.49. Found: C, 94.37; H, 5.57.

Acknowledgements

The authors would like to acknowledge the financial support from the Institute of Materials Research and Engineering (IMRE), Agency for Science, Technology and Research (A*STAR). This work was supported by the A*STAR Computational Resource Centre through the use of its high performance computing facilities.

Notes and references

1 R. Hodyss and J. L. Beauchamp, *Anal. Chem*., 2005, **77**, 3607-3610.
2 A. Popov, H. Chen, O. N. Kharybin, E. N. Nikolaev and R. G. Cooks, *Chem. Commun*., 2005, 1953-1955.
3 J. M. Sylvia, J. A. Janni, J. D. Klein and K. M. Spencer, *Anal. Chem.*, 2000, **72**, 5834-5840.
4 S. F. Hallowell, *Talanta*, 2001, **54**, 447-458.
5 C. Vourvopoulos and P. C. Womble, *Talanta*, 2001, **54**, 459-468.
6 M. Krausa and K. Schorb, *J. Electroanal. Chem.*, 1999, **461**, 10-13.
7 (a) E. Wallis, T. M. Griffin, N. Popkie, Jr., M. A. Eagan, R. F. McAtee, D. Vrazel and J. McKinly, *Proc. SPIE-Int. Soc. Opt. Eng.*, 2005, **5795**, 54-64; (b) G. A. Eiceman and J. A. Stone, *Anal. Chem*., 2004, **76**, 390A-397A.
8 (a) M. Wang, G. Zhang, D. Zhang, D. Zhu and B. Z. Tang, *J. Mater. Chem*., 2010, **20**, 1858; (b) S. J. Toal, K. A. Jones, D. Magde and W. C. Trogler, *J. Am. Chem. Soc*., 2005, **127**, 11661; (c) Y. Hong, M. Haeussler, J. W. Y. Lam, Z. Li, K. K. Sin, Y. Dong, H. Tong, J. Liu, A. Qin, R. Renneberg and B. Z. Tang, *Chem.-Eur. J*., 2008, **14**, 6428; (d) Y. Hong, H. Xiong, J. W. Y. Lam, M. Haessler, J. Liu, Y. Yu, Y. Zhong, H. H. Y. Sung, I. D. Williams, K. S. Wong and B. Z. Tang, *Chem.-Eur. J*., 2010, **16**, 1232; (e) Y. Liu, Y. Tang, N. N. Barashkov, I. S. Irgibaeva, J. W. Y. Lam, R. Hu, D. Birimzhanova, Y. Yu and B. Z. Tang, *J. Am. Chem. Soc*., 2010, **132**, 13951; (f) T. L. Andrew and T. M. Swager, *J. Am. Chem. Soc*., 2007, **129**, 7254.
9 (a) S. Kim, H. E. Pudavar, A. Bonoiu and P. N. Prasad, *Adv. Mater*. 2007, **19**, 3791; (b) J. Liu, J. W. Y. Lam and B. Z. Tang, *J. Inorg. Organomet. Polym. Mater*., 2009, **19**, 249; (c) W. C. Wu, C. Y. Chen, Y. Tian, S. H. Jang, Y. Hong, Y. Liu, R. Hu, B. Z. Tang, Y. T. Lee, C. T. Chen, W. C. Chen and A. K. Y. Jen, *Adv. Funct. Mater*., 2010, **20**, 1413; (d) M. Faisal, Y. Hong, J. Liu, Y. Yu, J. W. Y. Lam, A. Qin, P. Lu and B. Z. Tang, *Chem.-Eur. J*., 2010, **16**, 4266; (e) F. Mahtab, Y. Yu, J. W. Y. Lam, J. Liu, B. Zhang, P. Lu, X. Zhang and B. Z. Tang, *Adv. Funct. Mater*., 2011, **21**, 1733-1740.
10 (a) H. Zhou, J. Li, M. H. Chua, H. Yan and B. Z. Tang, J. Xu. *Polym. Chem*., 2014, **5**, 5628-5637; (b) J. Liu, Y. Zhong, P. Lu, Y. Hong, J. W. Y. Lam, M. Faisal,Y. Yu, K. S. Wong and B. Z. Tang, *Polym. Chem*., 2010, **1**, 426; (c) A. Qin, J. W. Y. Lam, L. Tang, C. K. W. Jim, H. Zhao, J. Sun and B. Z. Tang, *Macromolecules*, 2009, **42**, 1421-1424; (d) X.-M. Hu, Q. Chen, D. Zhou, J. Cao, Y.-J. He and B.-H. Han, *Polym. Chem.*, 2011, **2**, 1124-1128; (e) J. Li, J. Liu, J. W. Y. Lam and B. Z. Tang. *RSC Advances*, 2013, **3**, 8193.
11 (a) S. Yamaguchi and T. M. Swager, *J. Am. Chem. Soc*., 2001, **123**, 12087-12088; (b) S. Zahn and T. M. Swager, *Angew. Chem., Int. Ed.*, 2002, **41**, 4226-4230; (c) W. Thomas III, J. P. Amara, R. E. Bjork and T. M. Swager, *Chem. Commun*., 2005, 4572-4574; (d) A. Narayanan, O. P. Varnavsky, T. M. Swager and T. Goodson III, *J. Phys. Chem. C*, 2008, **112**, 881-884; (e) S. Chen, Q. Zhang, J. Zhang, J. Gu and L. Zhang, *SensorActuat. B-Chem*, 2010, **149**, 155-160; (f) A. Rose, Z. Zhu, C. F. Madigan, T. M. Swager and V. Bulovic, *Nature*, 2005, **434**, 876-879; (g) I. A. Levitsky, W. B. Euler, N. Tokranova and A. Rose, *Appl. Phys. Lett*., 2007, **90**, 041904; (h) Y. Long, H. Chen, Y. Yang, H. Wang, Y. Yang, N. Li, K. Li, J. Pei and F. Liu, *Macromolecules*, 2009, **42**, 6501-6509; (i) J. T. Sarah, and C. T. Willianm, *J. Mater. Chem*., 2006, **16**, 2871-2883; (j) H. Nie, Y. Zhao, M. Zhang, Y. Ma, M. Baumgarten and K. Müllen, *Chem. Commun*., 2011, **47**, 1234-1236; (k) J. L. Novotney, W. R. Dichtel, *ACS Macro Lett.,* 2013, **2**, 423-426; (l) X. Wu, H. Li, Y. Xu, B. Xu, H. Tong, L. Wang, *Nanoscale*, 2014, **6**, 2375–2380.
12 (a) J. S. Yang and T. M. Swager, *J. Am. Chem. Soc*., 1998, **120**, 5321-5322; (b) J. S. Yang and T. M. Swager, *J. Am. Chem. Soc*., 1998, **120**, 11864-11873; (c) H. Nie, Y. Zhao, M. Zhang, Y. Ma, M. Baumgarten and K. Müllen, *Chem. Commun*., 2011, **47**, 1234-1236; (d) H. Nie, G. Sun, M. Zhang, M. Baumgarten and K. Müllen, *J. Mater. Chem*., 2012, **22,** 2129-2132; (e) B.

View Article Online
DOI: 10.1039/C6PY01358A

Xu, Y. Xu, X. Wang, H. Li, X. Wu, H. Tong, L. Wang, *Polym. Chem*., 2013, **4**, 5056–5059; (f)

13 H. Zhou, Q. Ye, W. T. Neo, J. Song, H. Yan, Y. Zong, B. Z. Tang, T. S. A. Hor, J. Xu, *Chem. Commun*., 2014, **50**, 13785.

14 (a) W. Dong, Y. Pan, M. Fritsch, U. Scherf, *J. Polym. Sci. A: Polym. Chem.*, 2014, **53**, 1753-1761; (b) K. R. Ghosh, S. K. Saha, Z. Y. Wang, *Polym. Chem.*, 2014, **5**, 5638-5643; (c) R. Hu, J. L. Maldonado, M. Rodriguez, C. Deng, C. K. W. Jim, J. W. Y. Lam, M. M. F. Yuen, G. Ramos-Ortiz and B. Z. Tang. *J. Mater. Chem*., 2012, **22**, 232-240; (d) R. Hu, J. W. Y. Lam, J. Liu, H. H. Y. Sung, I. D. Williams, Z. Yue, K. S. Wong, M. M. F. Yuen and B. Z. Tang. *Polym. Chem*., **2012**, *3*, 1481-1489.

15 G.-F. Zhang, Z.-Q. Chen, M. P. Aldred, Z. Hu, T. Chen, Z. Huang, X. Meng, M.-Q. Zhu, *Chem. Commun*., 2014, **50**, 12058.

16 (a) M. P. Aldred, C. Li, G.-F. Zhang, W.-L. Gong, A. D. Q. Li, Y. Dai, D. Ma, M.-Q. Zhu, *J. Mater. Chem*., 2012, **22**, 7515–7528; (b) Q. Sun, H. Wang, C. Yang and Y. Li, *J. Mater. Chem*., 2003, **13**, 800.

17 (a) D. H. Reneker, A. L. Yarin, H. Fong, S. Koombhongse, *J. Appl. Phys.*, 2000, **87**, 4531-4547; (b) S. V. Fridrikh, J. H. Yu, M. P. Brenner, G. C. Rutledge, *Phys. Rev. Lett*., 2003, **90**, 144502. 1-4; (c) M. G. McKee, T. Park, S. Unal, I. Yilgor, T. E. Long, *Polymer*, 2005, **46**, 2011-2015; (d) D. Li, Y. Xia, *Adv. Mater*., 2004, **16**, 1151-1170.

18 (a) J. Liu, J. Fan, Z. Zhang, Q. Hu, T. Zeng and B. Li, *J. Colloid Interface Sci.*,2013, **394**, 386-393; (b) A. Tuteja, W. Choi, J. M. Mabry, G. H. McKinley and R. E. Cohen, *Proc. Natl. Acad. Sci. USA*, 2008, **105**, 18200-18205; (c) V. A. Ganesh, A. S. Nair, H. K. Raut, T. T. Y. Tan, C. He, S. Ramakrishna and J. Xu, *J. Mater. Chem*., 2012, **22**, 18479-18485; (d) A. Tuteja, W. Choi, M. Ma, J. M. Mabry, S. A. Mazzella, G. C. Rutledge, G. H. McKinley and R. E. Cohen, *Science*, 2007, **318**, 1618-1622.

19 (a) P. Gong, P. Xue, C. Qian, Z. Zhang, R. Lu, *Org. Biomol. Chem.*, 2014, **12**, 6134-6144; (b) H. Ma, L. Yao, P. Li, O. Ablikim, Y. Cheng, M. Zhang, *Chem. Eur. J.,* 2014, **20**, 11655-11658; (c) Z. Ding, Q. Zhao, R. Xing, X. Wang, J. Ding, L. Wang, Y. Han, *J. Mater. Chem. C*, 2013, **1**, 786-792; (d) T. Naddo, Y. Che, W. Zhang, K. Balakrishnan, X. Yang, M. Yen, J. Zhao, J. S. Moore, L. Zang, *J. Am. Chem. Soc.*, 2007, **129**, 6978-6979.

20 J. C. Sanchez, A. G. DiPasquale, A. L. Rheingold, W. C. Trogler, *Chem. Mater.,* 2007, **19**, 6459-6470.

View Article Online
DOI: 10.1039/C6PY01358A

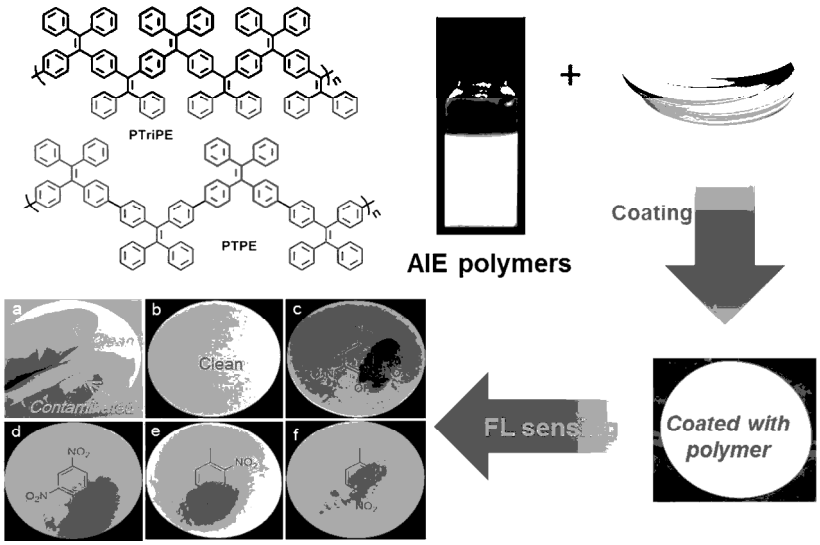

ABSTRACT:

This paper reports two structurally unique aggregation-induced emission (AIE) polymers that are fully constructed by AIE luminogen tetraphenyl or triphenyl ethene units. Their applications used for paper sensors are studied.